J. Neural Eng. **8** (2011) 065008 (12pp) doi:10.1088/1741-2560/8/6/065008

Single input optimal control for globally coupled neuron networks

Ali Nabi[1] **and Jeff Moehlis**

Department of Mechanical Engineering, University of California at Santa Barbara, Santa Barbara, CA 93106, USA

E-mail: nabi@engineering.ucsb.edu

Received 1 February 2011
Accepted for publication 8 June 2011
Published 4 November 2011
Online at stacks.iop.org/JNE/8/065008

Abstract

We consider the problem of desynchronizing a network of synchronized, globally (all-to-all) coupled neurons using an input to a single neuron. This is done by applying the discrete time dynamic programming method to reduced phase models for neural populations. This technique numerically minimizes a certain cost function over the whole state space, and is applied to a Kuramoto model and a reduced phase model for Hodgkin–Huxley neurons with electrotonic coupling. We evaluate the effectiveness of control inputs obtained by averaging over results obtained for different coupling strengths. We also investigate the applicability of this method to Hodgkin–Huxley models driven by multiplicative stimuli.

(Some figures in this article are in colour only in the electronic version)

1. Introduction

Due to their periodic spiking behavior, neurons are often thought of as oscillators whose state may be represented by a phase variable. Although phase models of neurons have been extensively used to investigate the patterns of synchrony that result from the type and architecture of coupling [1–7] and to characterize the response of large groups of oscillators to external stimuli [8–10], only recently have researchers used these phase models in the context of controlling neurons to achieve certain desired behavior [8, 11–18].

Much of the motivation for considering demand-control problems for neurons comes from the desire to increase the efficacy of surgical treatment of certain neurological diseases, like Parkinson's disease, by a method known as electrical deep brain stimulation (EDBS). In standard EDBS, a high-frequency (>100 Hz), low-duration (60–450 μs) mono-polar pulse train of up to 10.5 V is injected in the brain through a surgically implanted electrode to mitigate the pathological synchrony of populations of neurons, which is thought to be one of the potential causes of the disease [19–23]. Despite the fact that this method has shown substantial improvement in the condition of its receiving patients [19, 22, 23], an optimal (feedback-based) approach is attractive from a clinical perspective to optimize the timing and energy of the input stimulus, which would directly result in reducing the potential negative side effects of the procedure.

When it comes to controlling phase models of neurons, most of the work in the literature has been either on a single neuron level [8, 11–15, 17] or, if on the population level, multiple inputs have been allowed to the system [16, 24]. However, since there is typically only one electrode implanted into the brain, EDBS in its current state is limited by the number of input stimuli that it can deliver. This hinders the implementation of the previous methods in practice.

In recent work [18], we have proposed nonlinear hybrid control as a promising method for controlling networks of neurons with a single input. In this paper, we consider a different approach. Specifically, we employ discrete dynamic programming as an efficient mathematical optimization method for numerically solving the problem of desynchronizing a network of pathologically synchronized, globally (all-to-all) coupled phase neurons.

In dynamic programming, a cost function is defined that is to be minimized over the entire time horizon. From this cost function, one finds the value functions $V_1(x), V_2(x), \ldots, V_K(x)$ for all states $x \in \mathcal{X}^d$, where the indices $1, 2, \ldots, K$ represent time and $\mathcal{X}^d$ is the state space. These value functions indicate the *cost-to-go* from time k

[1] Author to whom any correspondence should be addressed.

at state x to the end time. Therefore, by computing the value functions, one has knowledge of the cost incurred for accomplishing a certain desired task starting from any point in the time domain and any point in the state space. The value functions are recursively computed by defining the value of the cost-to-go at time step $K+1$, $V_{K+1}(x)$.

The organization of the paper is as follows. In section 2, after giving the general form for phase models of networks of coupled neurons, we briefly introduce the Kuramoto model and then elaborate on deriving the Hodgkin–Huxley phase model for networks of coupled neurons. In section 3, we present the setup of the discretized model and explain, in detail, our control strategy in the dynamic programming framework. We present the results in section 4 along with some discussion. In section 5, we consider applying dynamic programming to a Hodgkin–Huxley phase model driven by a multiplicative control. Finally, in section 6, we draw conclusions and discuss some future directions.

2. The mathematical model

For a general network of N weakly coupled phase neurons (or, more generally, oscillators) we have [25]

$$\dot{\theta}_i = \omega_i + \sum_{j=1}^{N} \mathcal{F}_{ij}(\theta_j - \theta_i), \qquad i = 1, 2, \ldots, N,$$

where $\theta_i \in (0, 2\pi]$ is the phase of neuron i, ω_i is its natural frequency of spiking and $\mathcal{F}_{ij}(\cdot)$ is the 2π-periodic coupling function acting on neuron i from neuron j.

As mentioned earlier, we restrict the problem by only allowing a single control input, with the assumption that this control input is an additive control input that, without loss of generality, is applied to the Nth neuron in the network. Later, in section 5, we briefly explore the case of a multiplicative control as well. We also assume in this study that all neurons are identical and hence they all have identical natural frequencies ω, and that the functional form of the coupling between any pair of neurons is identical, but the strength of this coupling may be different. This yields the controlled form of the coupled phase neuron system as

$$\dot{\theta}_i = \omega + \sum_{j=1}^{N} \alpha_{ij} f(\theta_j - \theta_i) + \delta_{iN} u(t) \tag{1}$$

for $i = 1, 2, \ldots, N$. Here, we have assumed that $\mathcal{F}_{ij}(\cdot) \equiv \alpha_{ij} f(\cdot)$, where α_{ij} is the coupling strength from neuron j to neuron i, $f(\cdot)$ is the 2π-periodic coupling function acting between every pair of neurons, δ is the Kronecker delta function, and $u(t)$ is the single control input.

The coupling function $f(\cdot)$ distinguishes between different models. For the Kuramoto model, $f(\cdot) = \sin(\cdot)$, which yields

$$\dot{\theta}_i = \omega + \sum_{j=1}^{N} \alpha_{ij} \sin(\theta_j - \theta_i) + \delta_{iN} u(t). \tag{2}$$

This characterizes a system of globally heterogeneously coupled Kuramoto phase neurons driven by a single control input. We should mention that Kuramoto's phase model can be applied to many other oscillator systems and is not specific to neurons. Applications range from biology [26–29] to physics and engineering [30–34]. A good review on the Kuramoto model is given in [25].

For the rest of this section, we focus on deriving an example coupling function for Hodgkin–Huxley's model for neurons [35]. This model, presented in 1952, was derived to model Loligo squid's giant axon. Since it is the most widely used model in the literature for modeling the dynamics of neurons, we chose to consider it in the present study. The specifics of this model are as follows:

$$\begin{aligned}
\dot{V} &= (I_b + I(t))/c + \underbrace{(-\bar{g}_{Na} h (V - V_{Na}) m^3 - \bar{g}_K (V - V_K) n^4 - \bar{g}_L (V - V_L))}_{I_g(V,m,h,n)}/c, \\
\dot{m} &= a_m(V)(1 - m) - b_m(V) m, \\
\dot{h} &= a_h(V)(1 - h) - b_h(V) h, \\
\dot{n} &= a_n(V)(1 - n) - b_n(V) n,
\end{aligned} \tag{3}$$

where

$$\begin{aligned}
a_m(V) &= 0.1(V + 40)/(1 - \exp(-(V + 40)/10)), \\
b_m(V) &= 4 \exp(-(V + 65)/18), \\
a_h(V) &= 0.07 \exp(-(V + 65)/20), \\
b_h(V) &= 1/(1 + \exp(-(V + 35)/10)), \\
a_n(V) &= 0.01(V + 55)/(1 - \exp(-(V + 55)/10)), \\
b_n(V) &= 0.125 \exp(-(V + 65)/80), \\
V_{\mathrm{Na}} &= 50 \text{ mV}, \quad V_{\mathrm{K}} = -77 \text{ mV}, \quad V_L = -54.4 \text{ mV}, \\
\bar{g}_{\mathrm{Na}} &= 120 \text{ mS cm}^{-2}, \qquad \bar{g}_{\mathrm{K}} = 36 \text{ mS cm}^{-2}, \\
\bar{g}_L &= 0.3 \text{ mS cm}^{-2}, \qquad c = 1 \ \mu\text{F cm}^{-2},
\end{aligned}$$

in which $V \in \mathbb{R}$ is the voltage across the neuron membrane, $[m, h, n]^{\mathrm{T}} \in \mathbb{R}^3_{[0,1]}$ is the vector of *gating* variables which correspond to the state of the membrane's ion channels, $c \in \mathbb{R}^+$ is the constant membrane capacitance, $I_g : \mathbb{R} \times \mathbb{R}^3 \mapsto \mathbb{R}$ is the sum of the membrane currents and $I : \mathbb{R} \mapsto \mathbb{R}$ is the stimulus current. $I_b \in \mathbb{R}$ is the baseline current, which represents the effect of other parts of the brain on the neuron under consideration and can be viewed as a bifurcation parameter in the model that controls whether the neuron is in an excitable or an oscillatory regime. In, e.g., [36], it is discussed that in this model for $I_b < 6.26\ \mu\text{A cm}^{-2}$ the neuron would be in excitable mode where it does not show spontaneous periodic spiking. For $6.26 \leqslant I_b \leqslant 9.78\ \mu\text{A cm}^{-2}$, there is a bistable regime in which the neuron can be excitable or oscillatory, and for $I_b > 9.78\ \mu\text{A cm}^{-2}$, the neuron would be in oscillatory regime where it has a stable periodic orbit and oscillates with period $T_s < +\infty$. For $I_b = 10\ \mu\text{A cm}^{-2}$, which we will use in the following, the period of oscillations is $T_s = 14.63$ ms. In the oscillatory mode, the neuron periodically gives action potentials in the form of voltage spikes.

When grouped together, the spiking of each neuron affects the voltage dynamics of the neighboring neurons as they sense the spike as an input. This interaction is referred to as *electrotonic* coupling. It can be mathematically modeled by modifying the voltage equation in (3):

$$\dot{V}_i = (I_b + I_g + I(t))/c + \alpha_e \sum_{j=1}^{N} (V_j - V_i), \tag{4}$$

where α_e is the electrotonic coupling strength between the neurons. We assume that the network is weakly coupled and hence $\alpha_e = \mathcal{O}(\epsilon)$, where $\epsilon > 0$ is a small number. It should be pointed out that the effect of electrotonic coupling only manifests itself in the voltage dynamics and not in the dynamics of the gating variables [37]. We also note that the techniques that we consider in this paper could also be used for synaptic coupling, and in fact any type of coupling for which a phase reduction can be performed. We choose to consider electrotonic coupling for simplicity of presentation.

In order to find the reduced phase model [4, 38–40] for the Hodgkin–Huxley coupled neuron system, we first consider (3) in the absence of any external input stimulus $I(t)$. This system oscillates with period T. To characterize this oscillation, following [9, 41], a phase variable $\theta \in (0, 2\pi]$ is defined such that

$$\frac{\mathrm{d}\theta}{\mathrm{d}t} = \omega = \frac{2\pi}{T}.$$

Now, if we define $\mathbf{X} = [V, m, h, n]^{\mathrm{T}}$ as the state vector for the system, we can combine (3) and (4) and write the coupled system's equations as

$$\frac{\mathrm{d}\mathbf{X}_i}{\mathrm{d}t} = \mathbf{F}(\mathbf{X}_i) + \epsilon \sum_{j=1}^{N} \mathbf{p}(\mathbf{X}_i, \mathbf{X}_j)$$

for $i = 1, \ldots, N$. In this equation, $\mathbf{F}(\mathbf{X}_i)$ represents the dynamics of neuron i in the absence of any external stimuli or coupling effects and $\mathbf{p}(\mathbf{X}_i, \mathbf{X}_j)$ accounts for the effect that neuron j has on neuron i due to coupling. We can write [4]

$$\begin{aligned}\frac{\mathrm{d}\theta_i}{\mathrm{d}t} &= \frac{\partial\theta_i}{\partial\mathbf{X}_i} \cdot \frac{\mathrm{d}\mathbf{X}_i}{\mathrm{d}t} \\ &= \frac{\partial\theta_i}{\partial\mathbf{X}_i} \cdot \left(\mathbf{F}(\mathbf{X}_i) + \epsilon \sum_{j=1}^{N} \mathbf{p}(\mathbf{X}_i, \mathbf{X}_j)\right) \\ &= \omega + \epsilon \frac{\partial\theta_i}{\partial\mathbf{X}_i} \cdot \sum_{j=1}^{N} \mathbf{p}(\mathbf{X}_i, \mathbf{X}_j)\end{aligned}$$

for $i = 1, \ldots, N$. We note that in the absence of coupling terms, we obtain $\frac{\mathrm{d}\theta_i}{\mathrm{d}t} = \omega$, where we have assumed that all neurons have identical natural frequencies.

Since we have assumed weak coupling, we argue that each neuron, even under the influence of coupling, remains close to its stable periodic orbit that characterizes its periodic spiking in its phase space, i.e. $T \approx T_s$. In addition, there is a mapping from the states to the phase variable on the periodic orbit and so with the assumption of weak coupling (small ϵ), we can consider the effect of coupling as a perturbation to the oscillatory neuron and write

$$\frac{\mathrm{d}\theta_i}{\mathrm{d}t} = \omega + \epsilon \mathbf{Z}(\theta_i) \cdot \sum_{j=1}^{N} \mathbf{p}(\theta_i, \theta_j), \tag{5}$$

where $\mathbf{p}(\theta_i, \theta_j) = \mathbf{p}(\mathbf{X}_{po}(\theta_i), \mathbf{X}_{po}(\theta_j))$, with $\mathbf{X}_{po}$ denoting the periodic orbit. $\mathbf{Z}(\theta_i)$ represents the gradient of the phase variable θ_i with respect to the state variables $[V, m, h, n]^{\mathrm{T}}$ on the periodic orbit and is defined as

$$\mathbf{Z}(\theta_i) = \left.\frac{\partial\theta_i}{\partial\mathbf{X}_i}\right|_{\mathbf{X}_{po}(\theta_i)}.$$

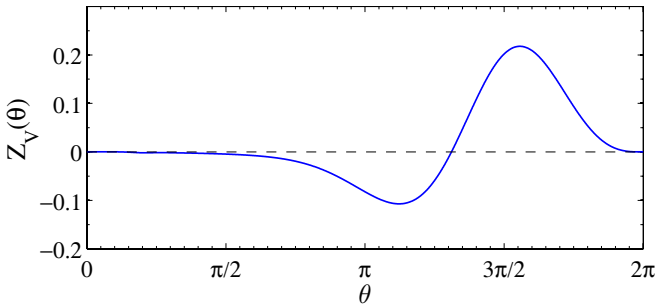

Figure 1. Hodgkin–Huxley PRC computed using the adjoint method as implemented by XPPAUT [42] with $I_b = 10\ \mu\mathrm{A\,cm^{-2}}$.

It turns out that since the coupling term $\mathbf{p}(\mathbf{X}_{po}(\theta_i), \mathbf{X}_{po}(\theta_j))$ is only dependent on the first state variable V (see (4)), only the first entry of $\mathbf{Z}(\theta_i)$ comes into play. This first entry, denoted by $Z_V(\theta_i)$, is called the phase response curve (PRC) of the ith neuron. For the Hodgkin–Huxley equations, $Z_V(\theta_i)$ can be computed numerically using the adjoint method; see, e.g., [9]. This can easily be done using the software XPPAUT available as open source software on the web [42, 43]. The PRC for the Hodgkin–Huxley equations is shown in figure 1. For notational convenience, we continue using the vector form of $\mathbf{Z}(\theta_i)$ in the equations.

We can simplify (5) by first defining $\theta_i = \phi_i + \omega t$. Substituting this into (5) one can take out the mean field effect of ω and write

$$\frac{\mathrm{d}\phi_i}{\mathrm{d}t} = \epsilon \mathbf{Z}(\phi_i + \omega t) \cdot \sum_{j=1}^{N} \mathbf{p}(\phi_i + \omega t, \phi_j + \omega t). \tag{6}$$

Using the averaging theorem from [44] and [45], we obtain the approximate equation

$$\frac{\mathrm{d}\phi_i}{\mathrm{d}t} = \frac{\epsilon}{T} \int_0^T \left[\mathbf{Z}(\phi_i + \omega\tau) \cdot \sum_{j=1}^{N} \mathbf{p}(\phi_i + \omega\tau, \phi_j + \omega\tau)\right] \mathrm{d}\tau.$$

Letting $s = \phi_i + \omega\tau$, we obtain

$$\frac{\mathrm{d}\phi_i}{\mathrm{d}t} = \frac{\epsilon}{2\pi} \sum_{j=1}^{N} \int_0^{2\pi} [\mathbf{Z}(s) \cdot \mathbf{p}(s, \phi_j - \phi_i + s)]\, \mathrm{d}s,$$

which in terms of θ_i is

$$\frac{\mathrm{d}\theta_i}{\mathrm{d}t} = \omega + \frac{\epsilon}{2\pi} \sum_{j=1}^{N} \int_0^{2\pi} [\mathbf{Z}(s) \cdot \mathbf{p}(s, \theta_j - \theta_i + s)]\, \mathrm{d}s. \tag{7}$$

It is worth pointing out that the right-hand sides of these equations are functions of the phase differences only. If we rewrite equation (7) more succinctly as

$$\frac{\mathrm{d}\theta_i}{\mathrm{d}t} = \omega + \alpha_e \sum_{j=1}^{N} f_e(\theta_j - \theta_i) \tag{8}$$

with $f_e(\cdot)$ denoting the electrotonic coupling, considering (4) and the fact that $\alpha_e = \mathcal{O}(\epsilon)$, we find $f_e(\cdot)$ to be

$$f_e(\theta) = \frac{1}{2\pi} \int_0^{2\pi} Z_V(s)(V_j(\theta + s) - V_i(s))\, \mathrm{d}s,$$

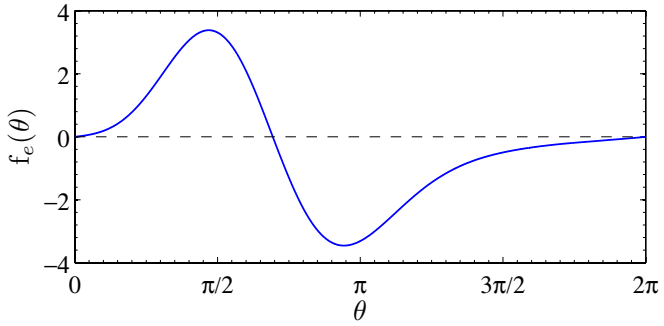

Figure 2. Electrotonic coupling function for the Hodgkin–Huxley equations with $I_b = 10\ \mu\text{A}\,\text{cm}^{-2}$.

where $Z_V(\cdot)$ is the PRC for the Hodgkin–Huxley equation as shown in figure 1. Figure 2 shows the plot of this coupling function computed numerically. $Z_V(\cdot)$ from figure 1 has been used in producing this figure.

In the presence of external control, an additional term would appear in (8) that would be a function of the external control stimulus $I(t)$ in (3), as we discuss more carefully in section 5. For now, we simplify the problem by considering the control input to be an additive $u(t)$ to (8) that incorporates the appropriate functional relationship with $I(t)$. Furthermore, we restrict the problem by only allowing a single control input to the system that, without loss of generality, is applied to the Nth neuron in the network. In order to incorporate heterogeneity of electrotonic coupling, instead of a common α_e, we consider different coupling strengths between different neuron pairs and rewrite (8) as

$$\frac{\mathrm{d}\theta_i}{\mathrm{d}t} = \omega + \sum_{j=1}^{N} \alpha_{ij} f_e(\theta_j - \theta_i) + \delta_{iN} u(t), \tag{9}$$

where δ_{iN} is the Kronecker delta function and u represents the control input. This equation is similar in form to (2), but with the coupling function being that shown in figure 2.

Now in order to further simplify the equations, we note that the right-hand sides of (2) and (9), and in general (1), are only in terms of phase differences. This allows us to find the phase difference dynamics for these systems and hence, by defining $\psi_i = \theta_i - \theta_1$ for $i = 2, 3, \ldots, N$, reduce the system dimension by 1. This yields the following general phase difference equations:

$$\dot{\psi}_i = \alpha_{i1} f(-\psi_i) - \alpha_{ii} f(0) + \sum_{j=2}^{N} [\alpha_{ij} f(\psi_j - \psi_i) - \alpha_{1j} f(\psi_j)] + \delta_{iN} u(t), \tag{10}$$

for $i = 2, 3, \ldots, N$. In these equations, $f(\cdot)$ can be any 2π-periodic coupling function. Equation (10) will be the basis on which we design and present the desynchronizing control law in subsequent sections.

3. Discretization and control

3.1. Discretization

In order to compute the desynchronizing control input for the system (10) numerically, we need to discretize these equations. To this end, we define $\mathrm{d}\psi$ to be the grid size for the phase differences ψ_i and $\mathrm{d}u$ to be the step size for the control input u. This yields the phase differences and control spaces $\psi_i^d = \{\mathrm{d}\psi, 2\,\mathrm{d}\psi, \ldots, 2\pi\}$ and $\mathcal{U}^d = \{-u_{\max}, \ldots, -\mathrm{d}u, 0, \mathrm{d}u, \ldots, u_{\max}\}$ for $i = 2, 3, \ldots, N$. We define the discrete state space $\mathcal{X}^d$ such that it has a state variable for every possible vector $(\psi_2, \psi_3, \ldots, \psi_N)$. Enumerating the states in the discrete state space yields $\mathcal{X}^d = \{1, 2, \ldots, n_{\mathcal{X}^d}\}$, where $n_{\mathcal{X}^d} = (\frac{2\pi}{\mathrm{d}\psi})^{N-1}$ is the total number of states. We assign the first state in $\mathcal{X}^d$ to the state $(\psi_2, \psi_3, \ldots, \psi_N) = (\mathrm{d}\psi, \mathrm{d}\psi, \ldots, \mathrm{d}\psi)$. Subsequent states in $\mathcal{X}^d$ are assigned to vectors of $(\psi_2, \psi_3, \ldots, \psi_N)$ in which, for $j = 2, \ldots, N-1$, each ψ_j increments by $\mathrm{d}\psi$ when ψ_{j+1} has finished marching through its minimum to its maximum with $\mathrm{d}\psi$ increments. This way, the $n_{\mathcal{X}^d}$ state of $\mathcal{X}^d$ corresponds to $(\psi_2, \psi_3, \ldots, \psi_N) = (2\pi, 2\pi, \ldots, 2\pi)$. At each instant of time, the state of the system is one of the states in the discrete state space $\mathcal{X}^d$. We choose $\mathrm{d}\psi$ to be a divisor of 2π to have an integer $n_{\mathcal{X}^d}$.

3.2. Discrete time dynamic programming

Considering (10), one can write the following general difference equation:

$$x_{k+1} = F_k(x_k, u_k) \qquad \forall k \in \{1, 2, \ldots, K\}, \tag{11}$$

where $x_k \in \mathcal{X}^d$ denotes the state of the system, corresponding to a case of $(\psi_2, \psi_3, \ldots, \psi_N)$, at time k, $u_k \in \mathcal{U}^d$ is the control input at time k, and $F_k(\cdot, \cdot)$ gives the dynamics of the system at time k computed by integrating the right-hand side of (10) numerically. K is the end time.

The objective is to find a sequence u_k for all $k \in \{1, 2, \ldots, K\}$, such that the state in (11) approaches a value for which the phase difference between any two neurons is at least as big as a predetermined amount $\Delta_{\min} \in [0, \frac{2\pi}{N}]$. The ideal case for desynchronizing the firing times for the population is when the state x in (11) approaches $x_{\text{splay}} = \{x | \psi_i \in \{\frac{2\pi}{N}, \frac{4\pi}{N}, \ldots, 2\pi\} \quad \psi_i \neq \psi_j \quad \forall i, j = 2, 3, \ldots, N, i \neq j\}$. For a system of N neurons, there are $(N-1)!$ splay states.

More concretely, we define the target set

$$\mathcal{X}_{\text{targ}} = \{x | (\psi_i \& (2\pi - \psi_i) \& |\psi_i - \psi_j|) > \Delta_{\min}\} \tag{12}$$

for all $i, j = 2, 3, \ldots, N$, $i \neq j$. If $x_K \in \mathcal{X}_{\text{targ}}$, then the system is considered to be desynchronized. In order to formulate the problem, we define the following time additive cost function:

$$J = \sum_{k=1}^{K} \gamma^2 u_k^2 + R(x_{K+1}), \tag{13}$$

where $\gamma > 0$ is a scalar penalizing factor and

$$R(x_{K+1}) = \left\| 1 + \sum_{i=2}^{N} \mathrm{e}^{\mathrm{j}\psi_{i,K+1}} \right\|. \tag{14}$$

Here $\mathrm{j} = \sqrt{-1}$ and the $\psi_{i,K+1}$ variables are the phase differences at time $K+1$ associated with state x_{K+1} as obtained from (11). $R(x_{K+1}) \in \mathbb{R}_{[0,N]}$ is known as the *end point cost*. The objective is to find a sequence $u_k \in \mathcal{U}^d$ for $k = \{1, 2, \ldots, K\}$ such that (13) is minimized subject to (11).

It is worth mentioning that $R(x_{K+1})$ is a variation of the order parameter for systems of coupled oscillators [25] rearranged to fit the phase difference system here and is minimized if the neurons desynchronize fully by assuming one of the splay states and maximized if the neurons synchronize. Therefore, by minimizing (13) along the solutions of (11) the state x is driven toward $x_{\text{splay}} \subset \mathcal{X}_{\text{targ}}$. We note that although reaching the splay state would be ideal in maximizing the ISIs, any state within the spectrum of in-phase and splay states may be achieved, and as long as the ISIs of the neurons are such that $x_K \subset \mathcal{X}_{\text{targ}}$, the system is considered desynchronized. Considering the bounded control, the values of the coupling strengths, the discretization error due to meshing the phase space, and the limited time of control application, it is likely that the optimal controller results in a final state that is not one of the splay states. Another point to make here is that by defining the cost function as in (13), we emphasize desynchronization at the last time step, K. By choosing K to correspond to the spiking instant of the population, one can hope for achieving desynchronization of spikes.

To cast the problem in the dynamic programming format, we argue that the cost presented in (13) is composed of the cost incurred from the current time step to the next, plus the *cost-to-go* from the next time step to the final time. The cost-to-go (also known as the *value function*) from a state x at time l, denoted as $V_l(x)$, can be written as follows [46]:

$$\begin{aligned} V_l(x) &= \inf_{u_k \in \mathcal{U}^d, \forall k \geqslant l} \left(\sum_{k=l}^{K} \gamma^2 u_k^2 + R(x_{K+1}) \right) \\ &= \inf_{u_k \in \mathcal{U}^d, \forall k \geqslant l} \left(\gamma^2 u_l^2 + \sum_{k=l+1}^{K} \gamma^2 u_k^2 + R(x_{K+1}) \right) \\ &= \inf_{u_l \in \mathcal{U}^d} \left(\gamma^2 u_l^2 + \inf_{u_k \in \mathcal{U}^d, \forall k \geqslant l+1} \left(\sum_{k=l+1}^{K} \gamma^2 u_k^2 + R(x_{K+1}) \right) \right). \end{aligned}$$

The inner infimum on the right-hand side of the above equation is exactly the cost-to-go starting at time $k = l + 1$ from the state $x_{l+1} = F_l(x, u_l)$. So we can write

$$V_l(x) = \inf_{u_l \in \mathcal{U}^d} \left(\gamma^2 u_l^2 + V_{l+1}(F_l(x, u_l)) \right) \tag{15}$$

for all $x \in \mathcal{X}^d$. This equation is valid for all $l \in \{1, 2, \ldots, K\}$ when we define

$$V_{K+1}(x) = \begin{cases} R(x_{K+1}) & \text{if} \quad x_{K+1} \in \mathcal{X}_{\text{targ}}, \\ +\infty & \text{if} \quad x_{K+1} \notin \mathcal{X}_{\text{targ}} \end{cases} \tag{16}$$

for all $x \in \mathcal{X}^d$. With this, the optimal control and trajectory will be

$$u_k^* = \arg \min_{u_k \in \mathcal{U}^d} \left(\gamma^2 u_k^2 + V_{k+1}(F_k(x_k^*, u_k)) \right), \tag{17}$$

$$x_{k+1}^* = F_k(x_k^*, u_k^*), \qquad x_1^* = x_1 \tag{18}$$

for all $k \in \{1, 2, \ldots, K\}$.

The final time K in the above formulation is chosen to be the time beyond which the control law would not be applied. We note that $x_{K+1} = F_k(x_K, u_K)$ and so if the state of the system is not going to fall within the set $\mathcal{X}_{\text{targ}}$ even by applying the optimum control at time K, u_K^*, then it is considered not to be desynchronizable and the cost-to-go that is associated with it for time step $K+1$ is infinity (see (16)). However, if with the control sequence $u_1^*, u_2^*, \ldots, u_K^*$ the system falls within the set $\mathcal{X}_{\text{targ}}$ at time $K+1$, then it would be considered desynchronized and a cost-to-go of $R(x_{K+1})$ is associated with it for time step $K + 1$. This formulation is known as *fixed termination time* dynamic programming.

3.3. Implementation in Matlab

Dynamic programming characterized by equations (15)–(18) forms a computationally efficient way to compute the cost-to-go for a system throughout the time and state domains recursively. After initializing $V_{K+1}(x)$, one can first perform a backward iteration to compute $V_1(x)$ for all $x \in \mathcal{X}^d$ [47]:

```
for k=K:-1:1
  V{k}=min(G{k}+V{k+1}(F{k}),[ ],2);
end
```

Then, given an initial condition $x(1)$, a forward iteration loop will yield the optimal control and state trajectories:

```
for k=1:K
  [dummy, u] = min(G{k}(x(k),:)+
                   V{k+1}(F{k}(x(k),:))',[ ],2);
  x(k+1) = F{k}(x(k),u);
end
```

4. Example

As an example, we solve this problem for a network of three neurons. In accordance with (10), we present the phase difference equations for a network of three neurons as

$$\begin{aligned} \dot{\psi}_2 &= -2\alpha_{12} \sin(\psi_2) + \alpha_{23} \sin(\psi_3 - \psi_2) - \alpha_{13} \sin(\psi_3), \\ \dot{\psi}_3 &= -2\alpha_{13} \sin(\psi_3) + \alpha_{23} \sin(\psi_2 - \psi_3) - \alpha_{12} \sin(\psi_2) + u \end{aligned} \tag{19}$$

for the Kuramoto system and

$$\begin{aligned} \dot{\psi}_2 &= \alpha_{12} \left(f_e(-\psi_2) - f_e(\psi_2) \right) \\ &\quad + \alpha_{23} f_e(\psi_3 - \psi_2) - \alpha_{13} f_e(\psi_3), \\ \dot{\psi}_3 &= \alpha_{13} \left(f_e(-\psi_3) - f_e(\psi_3) \right) \\ &\quad + \alpha_{23} f_e(\psi_2 - \psi_3) - \alpha_{12} f_e(\psi_2) + u \end{aligned} \tag{20}$$

for the Hodgkin–Huxley system. We note that we have assumed symmetry for the coupling strengths, i.e. $\alpha_{ij} = \alpha_{ji}$. The two splay states for this system are $(\psi_2, \psi_3) = \left(\frac{2\pi}{3}, \frac{4\pi}{3}\right)$ and $(\psi_2, \psi_3) = \left(\frac{4\pi}{3}, \frac{2\pi}{3}\right)$.

With positive values for α_{ij}, and in the absence of control, these systems synchronize resulting in $\psi_2 = \psi_3$ at all times. In order to find a desynchronizing control for these systems, one needs knowledge of α_{ij} values. Several experimental and numerical studies have been carried out to find these coupling strengths [48–53]. The values that are suggested in these studies generally fall within the range of $[0\,,\,1]$. Since the true values of the coupling strengths are unknown, we allow each α to change within this interval. For the purpose of simulations we consider $0.1 \leqslant \alpha_{ij} \leqslant 1$ with 0.1 steps. This gives ten possibilities for each α resulting in 1000 different combinations of $(\alpha_{12}, \alpha_{13}, \alpha_{23})$. We note that since we are

Table 1. The percentage of different $(\alpha_{12}, \alpha_{13}, \alpha_{23})$ cases for which a desynchronizing control law exists when employing fixed termination time dynamic programming with a synchronized initial condition. The simulations were performed for $T_f = 6.28$ time units with $dt = 0.0349$ for the Kuramoto system and $T_f = 14.6$ with $dt = 0.08$ for the Hodgkin–Huxley system. In these simulations $\Delta_{\min} = 10^\circ$ and $d\psi = 2^\circ$.

$u_{\max}$	Kuramoto	Hodgkin–Huxley
1	0%	30.7%
2	6.6%	61.1%
3	11.2%	77.7%

considering all-to-all coupling, we have omitted zero values for the coupling strengths. In addition, allowing different combinations for $(\alpha_{12}, \alpha_{13}, \alpha_{23})$ results in situations where the α values are very close to (or far from) each other, which resembles the different coupling strengths among an actual neural population.

To find the desynchronizing control law for (19) and (20), we apply the fixed termination time dynamic programming formulation and find the optimal control law for every case of $(\alpha_{12}, \alpha_{13}, \alpha_{23})$. Depending on the maximum allowable value for the control input $u_{\max}$ and the minimum acceptable phase difference $\Delta_{\min}$, a control sequence $u_1^*, u_2^*, \ldots, u_K^*$ can be found for some of the cases. This means that for those cases of $(\alpha_{12}, \alpha_{13}, \alpha_{23})$, a control input can be found that can achieve, for the system, a phase desynchronization of at least $\Delta_{\min}$. The simulations were carried out for $\Delta_{\min} = 10^\circ$ and using three different values for $u_{\max}$, namely $u_{\max} \in \{1, 2, 3\}$. The penalizing constant in (13) is taken to be $\gamma = 10^{-4}$. The statistics for the ratio of desynchronizable cases to the total number of cases (which is 1000) for both the Kuramoto system (19) and the Hodgkin–Huxley system (20) are shown in table 1. The period of control application was taken to be approximately equal to that of the uncontrolled neurons. The initial condition for all simulation results shown here is the synchronized state where $\psi_2 = \psi_3 = 2\pi$. As expected, table 1 shows an increase in the percentage of desynchronizable cases with the increase in control authority $u_{\max}$. We see that for $u_{\max} = 1$, there does not exist a control law that can desynchronize any of the 1000 different Kuramoto systems given the simulation parameters. We note that, according to table 1, it is easier to desynchronize the Hodgkin–Huxley model than the Kuramoto model. A possible explanation for this is that the slope of the coupling function at zero is smaller for the Hodgkin–Huxley model, which suggests that it would be easier for the control to drive the system away from the in-phase solution.

As an example, with $u_{\max} = 3$ and $\Delta_{\min} = 10^\circ$, figure 3(a) shows the end state $(\psi_2(K), \psi_3(K))$ for all different cases of $(\alpha_{12}, \alpha_{13}, \alpha_{23})$ for the Kuramoto model (19). Each case has been subject to its own optimal control input computed through fixed termination time dynamic programming, equations (13), (15) and (16). We note that multiple cases can end up at the same location in the state space. Figure 3(b) shows four planes in the α space with points shown for those cases that were desynchronized. Figure 4 communicates similar information for the Hodgkin–Huxley system (20). It can be seen from

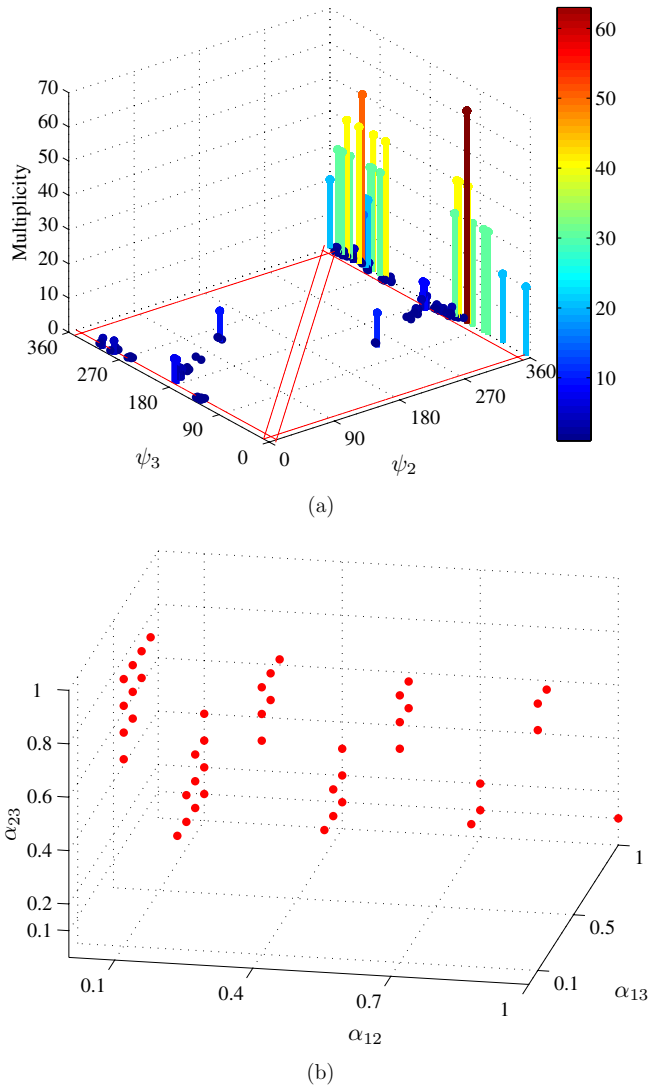

Figure 3. Simulation results for the Kuramoto system with $u_{\max} = 3$, $\Delta_{\min} = 10^\circ$ and $d\psi = 2^\circ$. (a) The end state $(\psi_2(K), \psi_3(K))$ for all different cases of $(\alpha_{12}, \alpha_{13}, \alpha_{23})$. Each case has been subjected to its own optimal control input computed through fixed termination time dynamic programming. (b) Four planes in the α space with points shown for those cases that were desynchronized.

figures 3(b) and 4(b) that as α_{12} increases, those $(\alpha_{12}, \alpha_{13}, \alpha_{23})$ combinations in which the α_{13} and α_{23} values are close to each other have a lesser chance of being desynchronized. This is intuitively appealing because the control is being applied to neuron 3 and so there needs to be a significant difference between the forces applied to neurons 1 and 2 (i.e., significant difference between α_{13} and α_{23}) for the control to even have a chance of overcoming the strong bond between neurons 1 and 2 (i.e., large α_{12}).

We have included the optimal control input and state trajectory obtained for the specific case of $(\alpha_{12}, \alpha_{13}, \alpha_{23}) = (0.1, 0.1, 0.7)$ with $\Delta_{\min} = 10^\circ$ and $u_{\max} = 3$ for both the Kuramoto and Hodgkin–Huxley systems in figures 5(a) and (b), respectively. As can be seen from these figures, the control has been able to take the system from the in-phase initial state to final states that are very close to the splay states.

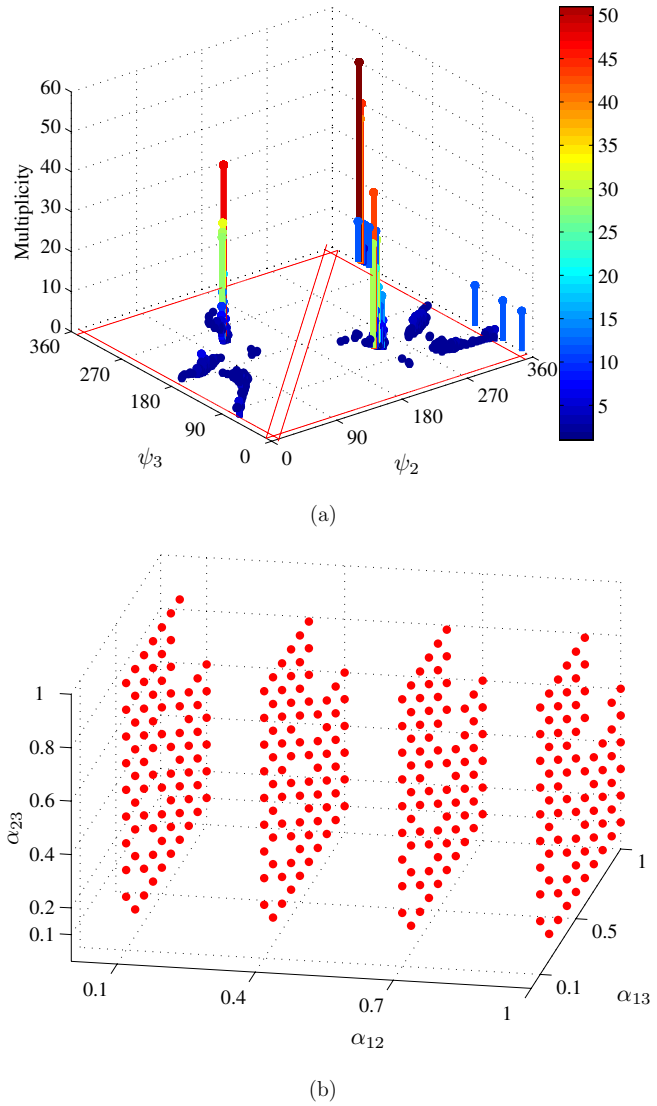

Figure 4. Simulation results for the Hodgkin–Huxley system with $u_{\max} = 3$, $\Delta_{\min} = 10^\circ$ and $d\psi = 2^\circ$. (a) The end state $(\psi_2(K), \psi_3(K))$ for all different cases of $(\alpha_{12}, \alpha_{13}, \alpha_{23})$. Each case has been subjected to its own optimal control input computed through fixed termination time dynamic programming. (b) Four planes in the α space with points shown for those cases that were desynchronized.

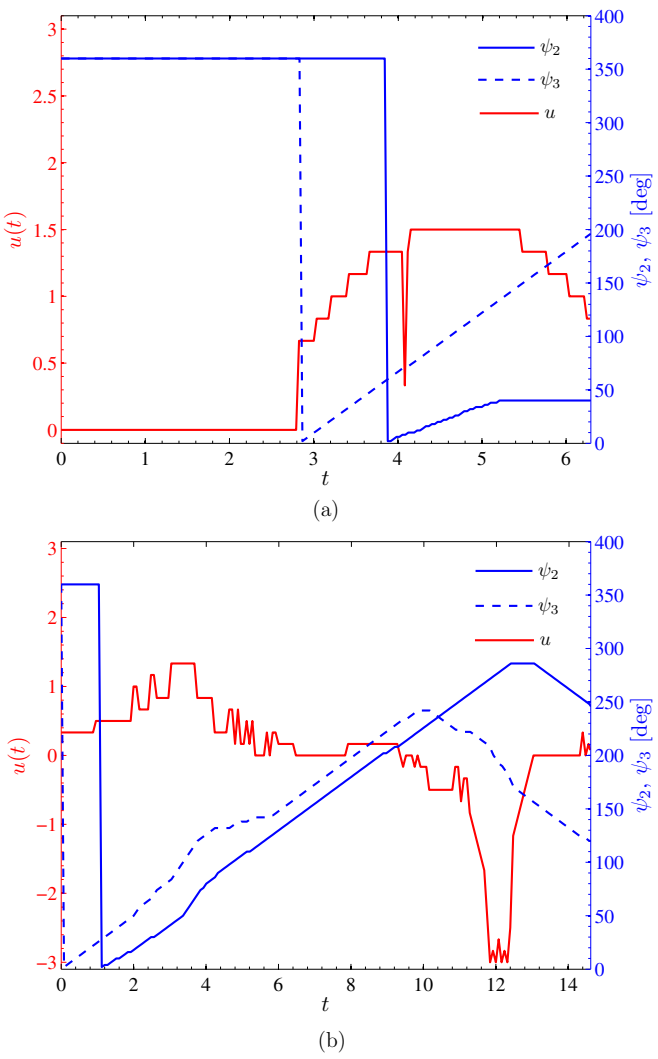

Figure 5. The optimal control input and state trajectory obtained for $(\alpha_{12}, \alpha_{13}, \alpha_{23}) = (0.1, 0.1, 0.7)$ with $u_{\max} = 3$, $\Delta_{\min} = 10^\circ$ and $d\psi = 2^\circ$ computed through fixed termination time dynamic programming for the (a) Kuramoto and (b) Hodgkin–Huxley systems.

We note that due to the way the cost function (13) is defined, for large enough simulation times, the resulting control stimulus would remain zero at first before it starts to apply force at some specific point in time. This is because of the fact that the time additive cost is only on the control input and the state cost only manifests itself at the last time step. As a result, the controller does not apply any control until there is just enough time to optimally desynchronize the system with an optimal control (see figure 5(a) for example).

One important point in finding a control law for networks of coupled neurons is that we may not have any knowledge about the coupling strengths α_{ij}. In order to find a more general solution, given a $u_{\max}$ and $\Delta_{\min}$, we might consider all the control inputs that are able to achieve desynchronization, feed them through an averaging filter, find the average control input and apply it to the entire 1000 different cases to investigate the probability of achieving desynchronization without having prior knowledge of coupling strengths. However, one can imagine that running a simple averaging routine on a number of different desynchronizing control sequences can result in an average sequence that is, due to potential cancellations, much smoother than each of the desynchronizing controls. This greatly reduces the chances of the averaged control in desynchronizing the network as it would, most likely, lack the important features of each control sequence.

In order to achieve a better averaged control stimulus for the general network, we first categorize the desynchronizing controls based on some *similarity index* and then find the average of each group. We then apply each of these averaged controls to the entire set of 1000 different cases and pick the one that results in the most desynchronizations as the best (final) answer. The similarity index for each desynchronizing control is a vector of length 10 that is obtained as follows. We divide the time axis of the control sequence into ten equal

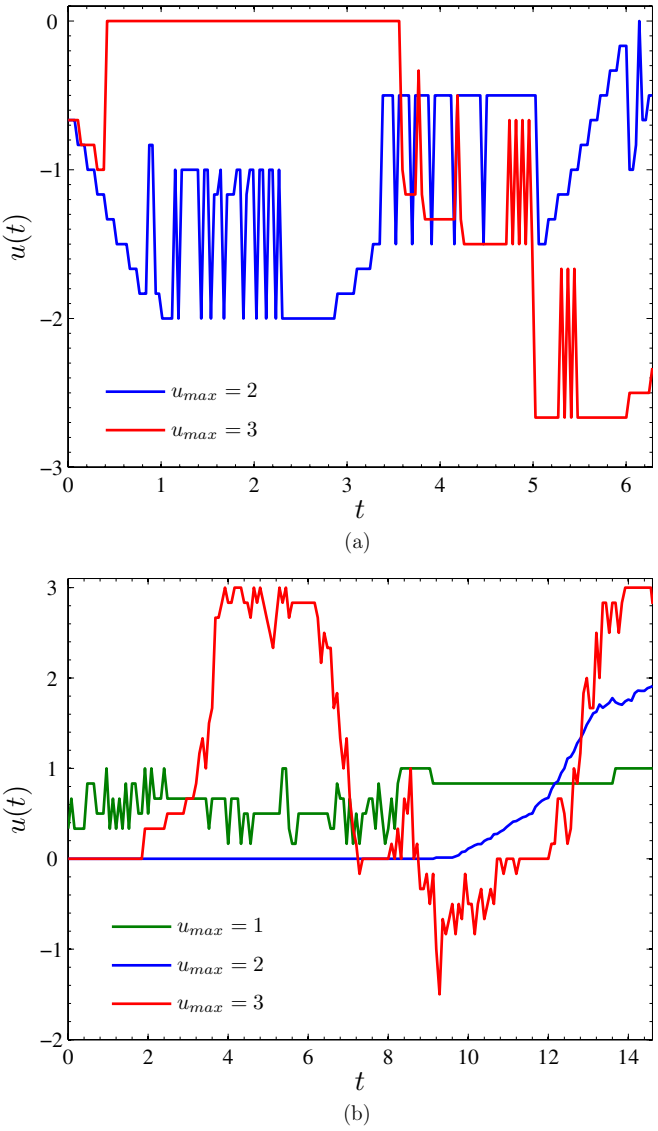

Figure 6. The averaged desynchronizing control inputs for different $u_{\max}$ values for (a) the Kuramoto system and (b) the Hodgkin–Huxley system. There does not exist a desynchronizing control with $u_{\max} = 1$ for the Kuramoto system.

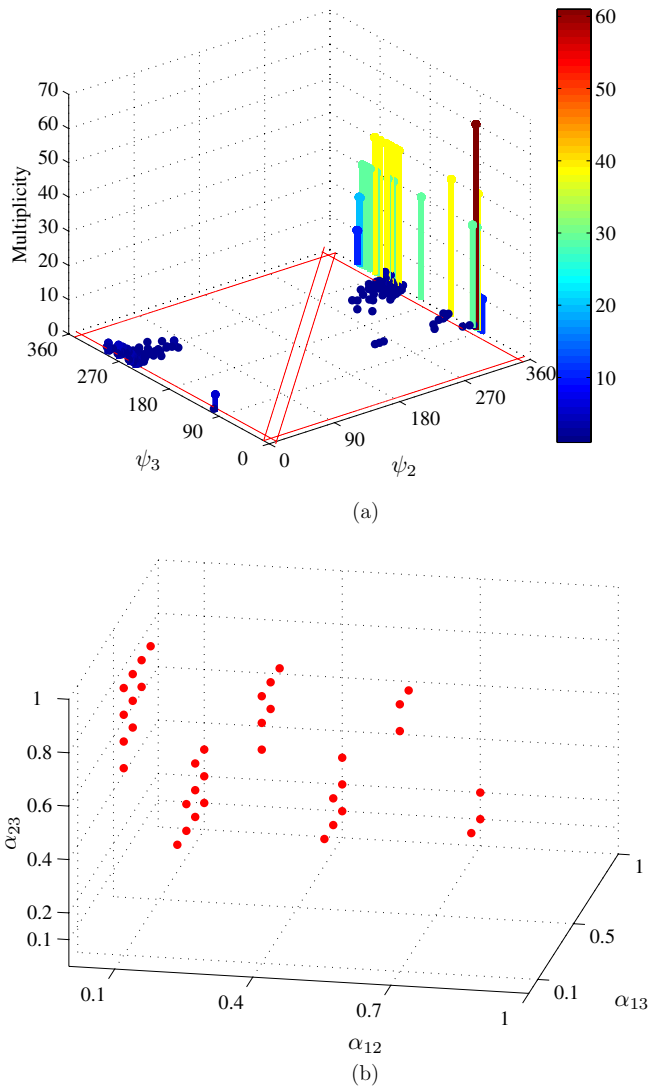

Figure 7. Simulation results for the Kuramoto system using the $u_{\max} = 3$ averaged control shown in figure 6(a) and with $\Delta_{\min} = 10^\circ$ and $d\psi = 2^\circ$. (a) The end state $(\psi_2(K), \psi_3(K))$ for all different cases of $(\alpha_{12}, \alpha_{13}, \alpha_{23})$. (b) Four planes in the α space with points shown for those cases that were desynchronized using the common averaged control. We see that for $\alpha_{12} = 1$ there are no desynchronized cases.

intervals. We find the mean value of the control sequence for each of these intervals. If the mean falls in $\left[\frac{u_{\max}}{2}, u_{\max}\right]$, we assign the number 2 to that interval. If the mean falls in $\left[0, \frac{u_{\max}}{2}\right)$, we assign the number 1 to that interval, if in $\left[-\frac{u_{\max}}{2}, 0\right)$, we assign -1 and if in $\left[-u_{\max}, -\frac{u_{\max}}{2}\right)$, we assign -2 to that interval. This way each desynchronizing control will have an index vector of length 10 where each entry is chosen from the set $\{-2, -1, 1, 2\}$. We then group all controls that have the same index vector.

The averaged desynchronizing control inputs for different values of $u_{\max}$ are shown in figure 6. The result of this investigation is summarized in table 2. The initial condition for all simulation results shown here is the synchronized state where $\psi_2 = \psi_3 = 2\pi$. To show the performance of the average controls, we have included figures 7 and 8 for the Kuramoto and Hodgkin–Huxley systems, respectively. These figures show simulation results for each of these systems using the $u_{\max} = 3$ averaged controls shown in figures 6(a) and (b).

Table 2. The probability of being able to desynchronize a synchronized network of three globally coupled neurons. The simulations were performed for $T_f = 6.28$ time units with $dt = 0.0349$ for the Kuramoto system and $T_f = 14.6$ with $dt = 0.08$ for the Hodgkin–Huxley system. In these simulations $\Delta_{\min} = 10^\circ$ and $d\psi = 2^\circ$. The control input for each simulation is found by averaging the desynchronizing control inputs.

$u_{\max}$	Kuramoto	Hodgkin–Huxley
1	0%	30.7%
2	4.9%	57.1%
3	8.4%	73.1%

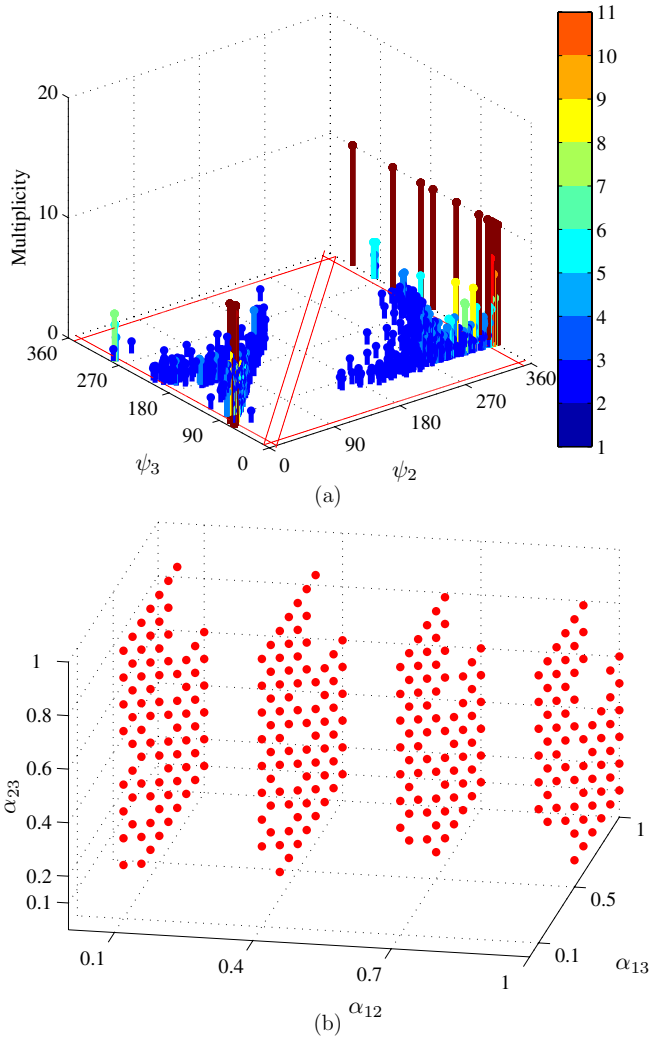

Figure 8. Simulation results for the Hodgkin–Huxley system using the $u_{\max} = 3$ averaged control shown in figure 6(b) and with $\Delta_{\min} = 10^\circ$ and $d\psi = 2^\circ$. (a) The end state $(\psi_2(K), \psi_3(K))$ for all different cases of $(\alpha_{12}, \alpha_{13}, \alpha_{23})$. (b) Four planes in the α space with points shown for those cases that were desynchronized using the common averaged control.

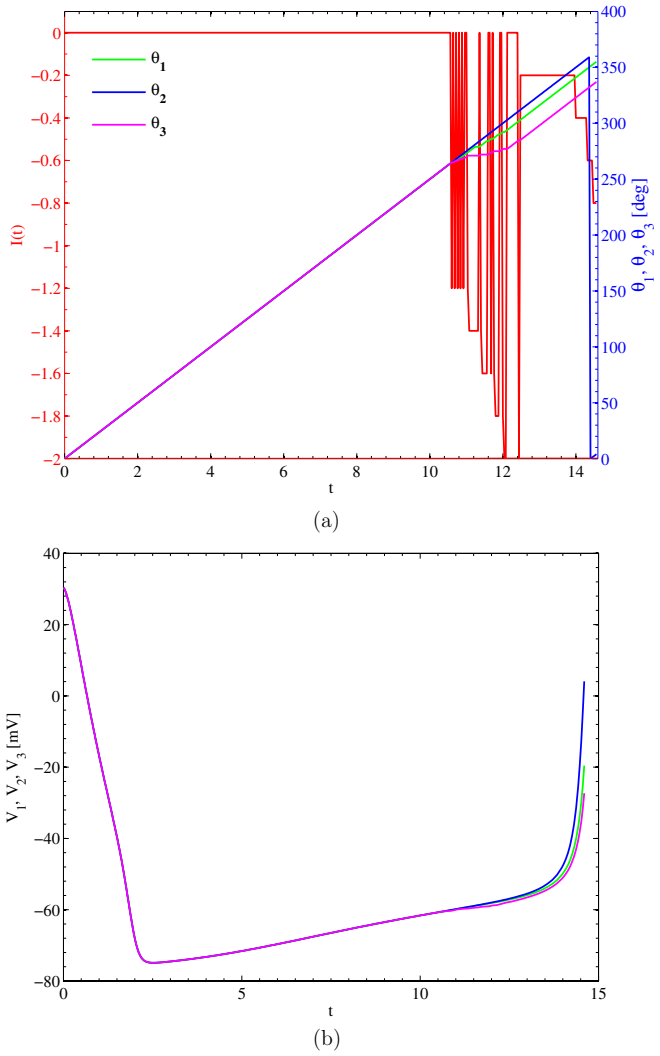

Figure 9. (a) The optimal control input (shown in red) and state trajectory obtained for $(\alpha_{12}, \alpha_{13}, \alpha_{23}) = (0.2, 0.6, 0.2)$ and $I_{\max} = 2\,\mu\text{A cm}^{-2}$ computed through fixed termination time dynamic programming for the Hodgkin–Huxley coupled phase model. (b) Voltage variable evolution for three coupled full Hodgkin–Huxley neurons under the control shown in (a). For this simulation, we have considered a mesh size of 1°.

5. Multiplicative control in the Hodgkin–Huxley phase model

In this section, we briefly investigate the control laws that one obtains by implementing dynamic programming on a different phase model for Hodgkin–Huxley neurons which allows a closer comparison to the full Hodgkin–Huxley model. In writing (1), we simplified the problem by assuming that the effect of the input current stimulus $I(t)$ on the phase dynamics is like an additive control $u(t)$. However, when one carefully does the phase reduction, the input current stimulus appears in the phase reduced model having been multiplied by the PRC of the neuron to which it is being applied, that is, $u(\theta, t) = Z_V(\theta_N) I(t)$. Indeed, using a generalization of the averaging theorem in [54] when $I(t) = \mathcal{O}(\epsilon)$, one can show that when the coupling **p** in (5) and the external input $u(\theta, t)$ are Lipschitz continuous in the state variables and continuous in time, on the time scale of $\mathcal{O}(1/\epsilon)$ the solutions of (6) can be approximated with the solutions for the system in which only the coupling term is averaged [55], cf [56]. So instead of (1) one obtains

$$\frac{d\theta_i}{dt} = \omega + \sum_{j=1}^{N} \alpha_{ij} f_e(\theta_j - \theta_i) + \delta_{iN} Z_V(\theta_i) I(t). \qquad (21)$$

We note that models of this form have been considered elsewhere, for example [8], but to our knowledge dynamic programming has not been applied to such a model before. A computational challenge is that (21) cannot be rewritten in terms of phase differences only, so it is necessary to discretize $\theta_1, \theta_2, \ldots, \theta_N$ separately, which leads to a dynamic programming problem with one more dimension than the analogous problem for additive control considered above.

For a network of three neurons, we have applied the fixed termination time dynamic programming formulation to find the optimal desynchronizing control law for (21)

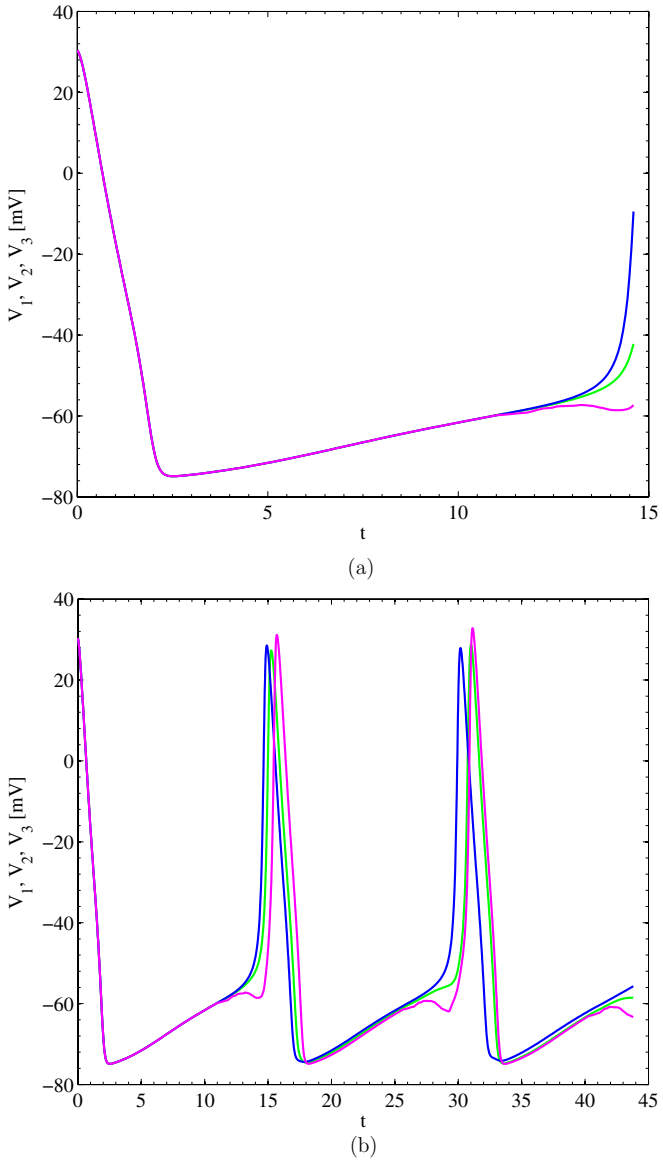

Figure 10. (a) Voltage traces for the full Hodgkin–Huxley model obtained for $(\alpha_{12}, \alpha_{13}, \alpha_{23}) = (0.2, 0.6, 0.2)$ by applying the optimal control input from the phase model (not shown) with $I_{\max} = 10\,\mu\text{A cm}^{-2}$ computed through fixed termination time dynamic programming. (b) Voltage traces as a result of applying three copies of the optimal input. For this simulation, we have considered a mesh size of 2°.

for the case of $(\alpha_{12}, \alpha_{13}, \alpha_{23}) = (0.2, 0.6, 0.2)$ and $I_{\max} = 2\,\mu\text{A cm}^{-2}$, with the results shown in figure 9(a). When this input is applied to the full model we see that the voltage traces of the three neurons become slightly desynchronized (figure 9(b)).

We have also found that when one increases the bound on $I(t)$ to $I_{\max} = 10\,\mu\text{A cm}^{-2}$, the resulting control only achieves a 2-1 state, in which two neurons have the same phase and the other has a different phase. It turns out that the algorithm determines that going to a 2-1 state that is spaced out on the phase circle results in less cost than going to any of the 1-1-1 states (in which all neurons have different phases) within the domain of capability of the control law. Interestingly, when the optimal control for this case is applied to the full Hodgkin–Huxley equations, it achieves an appreciable desynchronization (see figure 10).

We note that the major drawback for dynamic programming is that in this method the size of the state vector grows exponentially with the number of neurons in the system. Therefore, given one's computational power and resources, there are limitations as to how small the mesh size can be. In these simulations we have set the mesh size to be reasonably small, but we can still see the effect of the mesh size on the accuracy of the output results. For example, we have observed cases where, in the absence of any input, the weak coupling that should be acting as a synchronizing force for the neurons is actually unable to fully synchronize them. This is because as the phases of the neurons get closer to each other, the dynamical contribution from the coupling becomes smaller, eventually becoming so small that it is unable to exert enough force to move the neurons over the boundaries of their bins. An obvious future direction for this method would be to find efficient ways to perform these computations with reduced mesh size to avoid such issues in these systems. One observation that might help is that the computed controls that we find tend to be zero for the first half of the period of the neurons, starting right after they have fired. Intuitively, one can let the system evolve according to its natural dynamics until the control is needed and most effective. This suggests that we could start our initial condition at $\theta_1 = \theta_2 = \theta_3 = \pi$ at a time equal to half the period of the periodic orbit, assuming zero input for the evolution from $\theta_1 = \theta_2 = \theta_3 = 0$ (or 2π) up to this point, thereby freeing up computational resources for the consideration of smaller bins.

6. Conclusion and future directions

We have considered the problem of desynchronizing a network of pathologically synchronized globally coupled phase neurons using optimal control techniques. We used the Kuramoto model and a reduced phase model derived for a network of N Hodgkin–Huxley neurons under weak global electrotonic coupling as the basis for our control design. We allowed only one bounded control input to one of the neurons in the system, and we have assumed observability of all phases at all times. We introduced discrete dynamic programming as a mathematical optimization method for numerically solving this problem.

For both the Kuramoto and Hodgkin–Huxley models, the desynchronization problem was solved for a network of three coupled neurons. Since the coupling strengths between the neurons are in practice unknown, a spectrum of different coupling strengths was considered. For some combinations of coupling strengths there exists a desynchronizing control, while for some there does not. The period of control application was taken to be approximately equal to that of the uncontrolled neurons. The different desynchronizing control laws were then categorized and averaged, which resulted in a single control law for the entire system regardless of what the coupling strengths may be. When the bound on the controller is set to be $u_{\max} = 3$, this final control law can desynchronize the system, under

the mentioned assumptions and simulation parameters, with a probability of 8.4% for the Kuramoto network and 73.1% for the Hodgkin–Huxley network. Figure 6 and table 2 present the final control for each control bound and the probability of it achieving desynchronization.

The method was also tested with a more realistic modeling of the control for the Hodgkin–Huxley model. It was observed that there is good agreement between the simulation results and the theory on which the model is based. However, the curse of dimensionality and the effect of discretization error due to relatively large mesh size proved to be limiting factors that need more consideration in the future.

The control approach presented in this study can be viewed as an event-based control approach where the controller starts to apply input upon occurrence of an event. The event here would be the simultaneous spiking of all neurons. When the controller is triggered, it applies the precomputed traces of figure 6 and waits until the next event triggers it.

In order to improve the accuracy of the results presented in this paper, one can reduce the mesh size when discretizing the phases. This would substantially improve the precision of the solutions. However, by reducing the mesh size, the number of states grows exponentially, which can be detrimental given one's available computational power. We believe that by decreasing the mesh size, the results from the full Hodgkin–Huxley model will match more closely the results from the phase model presented in section 5. In addition, one can optimize the averaging process that leads to the final control laws, so that more systems, as characterized by their $(\alpha_{12}, \alpha_{13}, \alpha_{23})$, can be desynchronized with an averaged final control. Also, it would be beneficial to consider more combinations of $(\alpha_{12}, \alpha_{13}, \alpha_{23})$ in order to have a better probabilistic estimate for any control input.

The main drawback in dynamic programming is that it demands exponentially higher computational power as the number of states in the system is increased. An interesting future direction for this work would be to find reasonable approximations to networks of higher dimension to overcome the curse of dimensionality without greatly sacrificing the accuracy of the results. As a suggestion, one can think of splitting larger networks into several smaller networks that each are all-to-all coupled, but only communicate with each other through a mean field effect. This way, it might be possible to take advantage of parallel programming techniques and distribute the computational burden onto several processors.

Other interesting future directions would be to add uncertainties to the models and investigate the extent of the applicability of current control laws in the presence of noise and to compare the results obtained by dynamic programming to those for other control schemes.

Acknowledgments

This work was supported by the National Science Foundation grant NSF-1000678. The authors would like to thank João Hespanha for discussions related to this work, Mohammad Mirzadeh and Frederic Gibou for assistance in computations and the reviewers for their constructive comments.

References

[1] Cohen A, Holmes P and Rand R H 1982 The nature of coupling between segmental oscillators of the lamprey spinal generator for locomotion: a model *J. Math Biol.* **13** 345–69

[2] Kopell N and Ermentrout G B 1990 Phase transitions and other phenomena in chains of coupled oscillators *SIAM J. Appl. Math.* **50** 1014–52

[3] Ashwin P and Swift J 1992 The dynamics of N weakly coupled identical oscillators *J. Nonlinear Sci.* **2** 69–108

[4] Hansel D, Mato G and Meunier C 1993 Phase dynamics for weakly coupled Hodgkin–Huxley neurons *Europhys. Lett.* **25** 367–72

[5] Gerstner W, van Hemmen L and Cowan J 1996 What matters in neuronal locking? *Neural Comput.* **8** 1653–76

[6] Brown E, Holmes P and Moehlis J 2003 Globally coupled oscillator networks *Perspectives and Problems in Nonlinear Science: A Celebratory Volume in Honor of Larry Sirovich* ed E Kaplan, J Marsden and K R Sreenivasan (New York: Springer) pp 183–215

[7] Ghigliazza R M and Holmes P 2004 A minimal model of a central pattern generator and motoneurons for insect locomotion *SIAM J. Appl. Dyn. Syst.* **3** 671–700

[8] Tass P A 1999 *Phase Resetting in Medicine and Biology* (New York: Springer)

[9] Brown E, Moehlis J and Holmes P 2004 On the phase reduction and response dynamics of neural oscillator populations *Neural Comput.* **16** 673–715

[10] Brown E, Moehlis J, Holmes P, Clayton E, Rajkowski J and Aston-Jones G 2004 The influence of spike rate and stimulus duration on noradrenergic neurons *J. Comput. Neurosci.* **17** 13–29

[11] Moehlis J, Shea-Brown E and Rabitz H 2006 Optimal inputs for phase models of spiking neurons *ASME J. Comput. Nonlinear Dyn.* **1** 358–67

[12] Danzl P and Moehlis J 2007 Event-based feedback control of nonlinear oscillators using phase response curves *Proc. 46th IEEE Conf. on Decision and Control (New Orleans, LA)* pp 5806–11

[13] Danzl P and Moehlis J 2008 Spike timing control of oscillatory neuron models using impulsive and quasi-impulsive charge-balanced inputs *Proc. 2008 American Control Conf. (Seattle, WA)* pp 171–6

[14] Ullah G and Schiff S J 2009 Tracking and control of neuronal Hodgkin–Huxley dynamics *Phys. Rev.* E **79** 040901

[15] Schöll E, Hiller G, Hövel P and Dahlem M A 2009 Time-delayed feedback in neurosystems *Phil. Trans. R. Soc.* A **367** 1079–96

[16] Danzl P, Nabi A and Moehlis J 2010 Charge-balanced spike timing control for phase models of spiking neurons *Discrete Continuous Dyn. Syst.* A **28** 1413–35

[17] Nabi A and Moehlis J 2009 Charge-balanced optimal inputs for phase models of spiking neurons *Proc. 2009 ASME Dynamic Systems and Control Conf. (Hollywood, CA)* pp 685–7

[18] Nabi A and Moehlis J 2010 Nonlinear hybrid control of phase models for coupled oscillators *Proc. 2010 American Control Conf.* (*Baltimore, MD*) pp 922–3

[19] Deep Brain Stimulation for Parkinson's Disease Study Group 2001 Deep-brain stimulation of the subthalamic nucleus or the pars interna of the globus pallidus in Parkinson's disease *N. Engl. J. Med.* **345** 956–63

[20] Mayberg H S, Lozano A M, Voon V, McNeely H E, Seminowicz D, Hamani C, Schwalb J M and Kennedy S H 2005 Deep brain stimulation for treatment-resistant depression *Neuron* **45** 651–60

[21] Perlmutter J S and Mink J W 2006 Deep brain stimulation *Annu. Rev. Neurosci.* **29** 229–57
[22] Groiss S J, Wojtecki L, Südmeyer M and Schnitzler A 2009 Review: deep brain stimulation in Parkinson's disease *Therapeutic Adv. Neurological Disorders* **2** 379–91
[23] Breit S, Schulz J B and Benabid A L 2004 Deep brain stimulation *Cell Tissue Res.* **318** 275–88
[24] Tass P 2003 A model of desynchronizing deep brain stimulation with a demand-controlled coordinated reset of neural subpopulations *Biol. Cybern.* **89** 81–8
[25] Strogatz S H 2000 From Kuramoto to Crawford: exploring the onset of synchronization in populations of coupled oscillators *Physica* D **143** 1–20
[26] Michaels D C, Matyas E P and Jalife J 1987 Mechanisms of sinoatrial pacemaker synchronization: a new hypothesis *Circ. Res.* **61** 704–14
[27] Buck J 1988 Synchronous rhythmic flashing of fireflies: II *Q. Rev. Biol.* **63** 265–89
[28] Buck J and Buck E 1976 Synchronous fireflies *Sci.Am.* **234** 74–85
[29] Walker T J 1969 Acoustic synchrony—2 mechanisms in snowy tree cricket *Science* **166** 891
[30] Buck J and Buck E 1993 Numerical simulation of a large number of coupled lasers *J. Opt. Soc. Am.* **10** 155–63
[31] Kourtchatov S Yu, Likhanskii V V, Napartovich A P, Arecchi F T and Lapucci A 1995 Theory of phase locking of globally coupled laser arrays *Phys. Rev.* A **52** 4089–94
[32] York R A and Compton R C 1991 Quasi-optical power combining using mutually synchronized oscillator arrays *IEEE Trans. Microw. Theory Tech.* **39** 1000–9
[33] Wiesenfeld K, Colet P and Strogatz S H 1996 Synchronization transitions in a disordered Josephson series array *Phys. Rev. Lett.* **76** 404–7
[34] Wiesenfeld K, Colet P and Strogatz S H 1998 Frequency locking in Josephson arrays: connection with the Kuramoto model *Phys. Rev. E* **57** 1563–9
[35] Hodgkin A L and Huxley A F 1952 A quantitative description of membrane current and its application to conduction and excitation in nerve *J. Physiol.* **117** 500–44
[36] Moehlis J 2006 Canards for a reduction of the Hodgkin–Huxley equations *J. Math. Biol.* **52** 141–53
[37] Johnston D and Wu S M-S 1995 *Foundations of Cellular Neurophysiology* (Cambridge, MA: MIT Press)
[38] Winfree A 1974 Patterns of phase compromise in biological cycles *J. Math. Biol.* **1** 73–95
[39] Kuramoto Y 1984 *Chemical Oscillations, Waves and Turbulence* (New York: Springer)
[40] Winfree A 2001 *The Geometry of Biological Time* 2nd edn (New York: Springer)
[41] Guckenheimer J 1975 Isochrons and phaseless sets *J. Math. Biol.* **1** 259–73
[42] Ermentrout G B XPP-AUT. Available at http://www.math.pitt.edu/bard/xpp/xpp.html
[43] Ermentrout G B 2002 *Simulating, Analyzing and Animating Dynamical Systems: A Guide to XPPAUT for Researchers and Students* (Philadelphia, PA: SIAM)
[44] Guckenheimer J and Holmes P J 1983 *Nonlinear Oscillations, Dynamical Systems and Bifurcations of Vector Fields* (New York: Springer)
[45] Khalil H K 2002 *Nonlinear Systems* (Upper Saddle River, NJ: Prentice-Hall)
[46] Kirk D E 1970 *Optimal Control Theory: An Introduction* (New York: Dover)
[47] Hespanha J 2007 *An Introductory Course in Noncooperative Game Theory* (Santa Barbara, CA: University of California)
[48] Sherman A and Rinzel J 1992 Rhythmogenic effects of weak electrotonic coupling in neuronal models *Proc. Natl Acad. Sci. USA* **89** 2471–4
[49] Blankenship J E and Haskins J T 1979 Electrotonic coupling among neuroendocrine cells in aplysia *J. Neurophysiol.* **42** 347–55
[50] Ermentrout G B, Wang J W, Flores J and Gelperin A 2001 Model for olfactory discrimination and learning in limax procerebrum incorporating oscillatory dynamics and wave propagation *J. Neurophysiol.* **85** 1444–52
[51] Zhang X L, Zhang L and Carlen P L 2004 Electrotonic coupling between stratum oriens interneurons in the intact *in vitro* mouse juvenile hippocampus *J. Physiol.* **558** 825–39
[52] Mann-Metzer P and Yarom Y 1999 Electrotonic coupling interacts with intrinsic properties to generate synchronized activity in cerebellar networks of inhibitory interneurons *J. Neurosci.* **19** 3298–306
[53] Levavi-Sivan B, Bloch C L, Gutnick M J and Fleidervish I A 2005 Electrotonic coupling in the anterior pituitary of a teleost fish *Endocrinology* **146** 1048–52
[54] Sanders J A and Verhulst F 2007 *Averaging Methods in Nonlinear Dynamical Systems* 2nd edn (New York: Springer)
[55] Schmidt G S, Moehlis J and Allgöwer F 2011 in preparation
[56] Kori H, Kawamura Y, Nakao H, Arai K and Kuramoto Y 2009 Collective phase description of coupled oscillators with general network structure *Phys. Rev.* E **80** 036207